Edge Formation in High-Speed Intermittent Slot-Die Coating of Disruptively Stacked Thick Battery Electrodes

Ralf Diehm, Hannes Weinmann, Jana Kumberg, Marcel Schmitt, Jürgen Fleischer, Philip Scharfer, and Wilhelm Schabel*

In industrial lithium-ion battery manufacturing, patterned structured electrodes are required due to subsequent processes. In particular, novel and advanced cell stack formation processes cause challenging design requirements for electrode geometry. This work examines the influence of coating speeds up to 50 m min^{-1} and wet-film thicknesses up to 400 µm on the coating edge quality. To determine the coating edge quality, the start-up length in every pattern in the coating direction is compared for different coating parameters. Parameters such as speed and film thickness show no limiting effect, which makes high process speeds possible.

1. Introduction

Since the commercialization of lithium-ion batteries (LIBs), the mobility sector as an application field has moved to the focus of attention.[1] The reason can be due to the growing markets of electric vehicles (EVs), hybrid electric vehicles (HEVs), and plug-in hybrid electric vehicles (PHEVs). Mainly driven by falling battery costs and the need for local emission-free vehicles,[2] studies showed a need of more than 1 TWh of production capacity by 2025, which represents a significant increase.[3]

Depending on the cell stacking processes, there are different requirements for the electrode coating geometry. Basically, stacking processes can be divided into two main categories, namely, continuous and discontinuous processes.[4] The continuous processes include winding and Z-folding, whereas the discontinuous processes include Z-folding with single sheets and single-sheet stacking.[5] New stacking processes, such as the Helix folding process, require intermittent coating and place direct and demanding boundary conditions on the coating technology. Here, the quality of the cell stack directly depends on the coating quality since no cutting of the electrode web is possible in the Helix process.[6]

R. Diehm, J. Kumberg, Dr. M. Schmitt, Dr. P. Scharfer, Prof. W. Schabel
Karlsruhe Institute of Technology (KIT)
Institute of Thermal Process Engineering (TVT)
Thin Film Technology (TFT)
Kaiserstraße 12, Karlsruhe 76131, Germany
E-mail: ralf.diehm@kit.edu

H. Weinmann, Prof. J. Fleischer
Karlsruhe Institute of Technology (KIT)
wbk Institute of Production Science
Kaiserstraße 12, Karlsruhe 76131, Germany

The ORCID identification number(s) for the author(s) of this article can be found under https://doi.org/10.1002/ente.201900137.

DOI: 10.1002/ente.201900137

For those uncoated areas, the coating process must be interrupted in the web direction for a defined length. Intermittent slot-die coating can create this interruption and is widely used in industrial battery production. However, the time-consuming interruption process is a speed-limiting process for electrode manufacturing, and the coating quality of the electrode is also significant for cell performance. Mohanty et al. and David et al. have shown the influence of coating defects on the electrochemical performance and degradation mechanism in LIBs.[7,8] For intermittent coating, the edges at the beginning of the coating (rising edge) and at the end of the coating (falling edge) are important for the reliable functioning of the electrode and to keep the scrap rate to a minimum.[9] Yang et al. and Schmitt et al. have studied the defect formation and found that the defect formation mechanism is the same for the intermittent slot-die coating and for the regular continuous slot-die coating.[10,11] They have also found that precise control of fluid supply and coating speed is very important for intermittent coating. De Vries et al. examined the possibility of intermittent coating for low-viscous fluids and found that the film breakup mechanism is decisive for the quality of the edges.[12] Schmitt et al. studied the relationship between coated wet-film thickness (WFT) and slot-die pressure distribution and showed that a fine-tuned pressure distribution is important for uniformity of the coating in the web direction.[11] Diehm et al. have shown the potential of high-speed intermittent coating and the influence of viscosity and coating gap.[13,14] Chang et al. have studied the influence of fluid parameters and the coating setup on the start-up time of slot-die coating.[15] Maza and Carvalho investigated the formation of the falling edge and the influence of different geometries of the slot-die lips.[16]

So far, there are only few publications, which address the formation of the edges in the coating direction of intermittent coating. In this study, we want to show the influence of the two process parameters coating speed and WFT on the intermittent slot-die coating. The focus is on the shape and length of the rising and falling edges. Based on the experimental results, a model for the mechanism of the falling-edge formation is presented.

2. Results and Discussions

The aim of this work is to examine the relationship between coating speed and WFT on the one hand and edge quality on the other hand. Due to the goal of a precise intermittent coating,

the coating-edge quality is represented by the length of the rising and falling edges in the web direction. A representative such as waterborne LIB anode slurry with 43% solids was mixed and used for the experiments. A slot-die coating system was used to coat the battery slurry intermittently as rectangle patterns onto a rotating drum. After coating, the wet film was analyzed with an online 2D laser triangulation system to obtain a 3D profile of the applied film. The setup is described in the Experimental Section.

2.1. Coating Requirements for Stacking Methods with High Material Requirements

Helix is based on the zigzag folding process of intermittently coated electrode webs. Due to the small bending radii, the folding line must be uncoated to prevent the coating from flaking off.[6] The double-sided and intermittently coated anode web is guided between two separator webs and folded with the cathode web. The cathode runs 90° offset to the three material webs (separator–anode–separator); it is also intermittently coated but only single-sided,[6] as shown in **Figure 1**.

The sequence for stack formation starts with the three material webs (separator–anode–separator) to be laid down once. The cathode is then placed over this layer structure and folded back again directly so that the three material webs can be placed over it again. This alternating layer structure is carried out up to the desired stacking height.

The Helix folding process places direct and particularly high demands on the coating quality, as the cell stack is formed without further cutting processes. To maximize the energy density of the cell, the uncoated folding area must also be kept as small as possible.[6] Since the uncoated part of the electrode with both the rising edge and the falling edge is built into the cell, the length of the edges should be as small as possible to prevent unbalancing of the cell. The requirements of the Helix folding process places to the coating quality can be summarized, as shown in **Table 1**.

The challenge of the process lies in the simultaneous guidance of several material webs. Inadequate coating quality significantly complicates this process and leads to inaccuracies in the cell stack. **Figure 2** shows the coating on both sides that does not coincide. In case of such a coating error, no subsequent compensation by the process technology during stack formation is possible, since only alignment to one of the two coating sides is possible. Therefore, the electrodes with un-matching coatings would be off-spec material, significantly increasing the scrap rate of the overall manufacturing process.

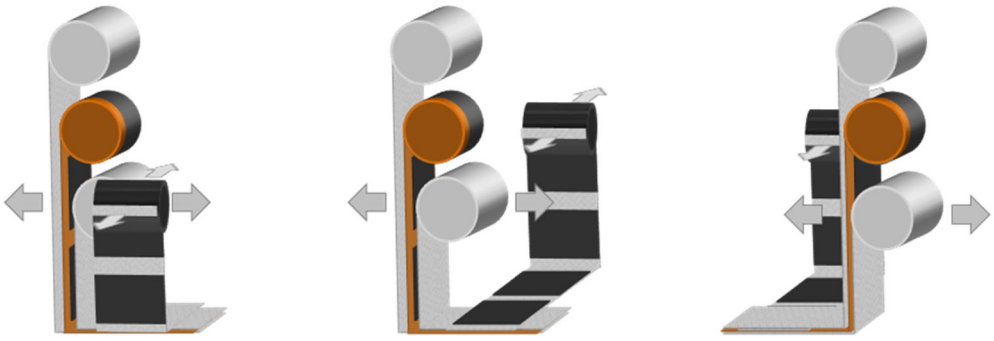

Figure 1. Schematic representation of the Helix folding process.

Table 1. Summary of requirements of the Helix folding process places to the coating quality.

Position	Orientation	Elevation	Linearity edge	Coating overlap
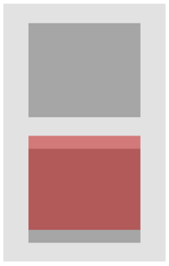		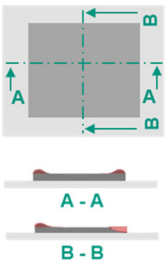		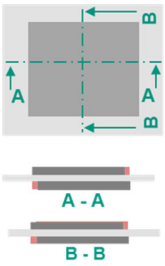
Spacings between the coating patterns are irregular, causing the uncoated folded film area to vary in length.	The coating edge is not at right angles to the foil edge, so that the patterns do not overlap during the folding process.	A raised starting edge and elevations at the coating edges add up over the layer structure and lead to beads on the cell stack.	The start and stop edges are not linear, which can lead to missing overlaps with the opposite electrode.	The coating of the anode coated on both sides is not congruent, which can lead to missing overlaps with the opposite cathode.

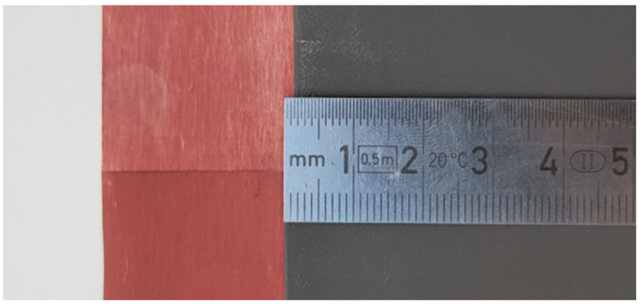

Figure 2. Example of an offset of the coatings on both sides of the current collector. This offset can lead to worse cell performance or direct scrap.

2.2. Slurry and Coating Properties

The mixing procedure of the anode slurry is described in the Experimental Section. The mixed slurry shows a strong shear-thinning behavior with a viscosity of 9 Pa s at 0.01 s^{-1} and 0.22 Pa s at 1000 s^{-1}, as shown in **Figure 3**. In this work, the applied shear rates range from 0 s^{-1} during the coating process to a maximum of 3106 s^{-1}.

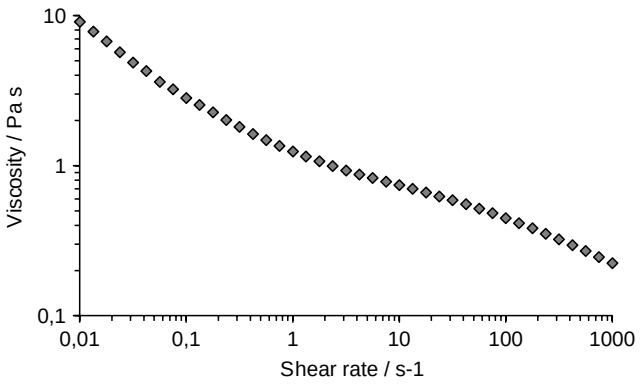

Figure 3. Average viscosity of the applied LIB anode slurry as a function of the applied shear rate. The slurry shows a strong shear-thinning behavior toward higher shear rates.

The maximum value of the shear rate depends on the coating gap width and the coating speed (**Table 2**). The highest shear rates and thus the lowest viscosity appear in the coating gap between the moving substrate and the fixed slot-die lips.

The resulting volume flow, as shown in Table 2, is calculated as the product of WFT, coating width, and coating speed. The layer thicknesses differ slightly at different coating speeds and WFT, since no mass-flow controller or feedback loop from the layer thickness was used. The differences in WFT for intermittent coating compared with continuous coating are described in the study by Schmitt et al.[11] With an increase in the coating speed, the capillary number, which describes the ratio of viscous to capillary forces, does not increase linearly (Table 2). The increase in the capillary number due to the coating speed is counteracted by the shear-thinning behavior of the paste and leads to a reduction in viscosity at higher coating speeds.

A picture with the example of an intermittent coating including rising edge, falling edge, and noncoating between the coating pattern is shown in **Figure 4**.

2.3. Influence of Coating Speed on Rising and Falling Edge

The influence of the coating speed on the edge quality is of decisive importance for the throughput increase. The maximum coating speed is limited by the quality requirements of the application, which is also addressed in this work. The normalized film profile in the web direction for a gap of 161 µm is shown in **Figure 5** for different web speeds from 10 up to 50 m min^{-1}.

After noncoating of 40 mm, the film profile rises sharply and reaches the steady state WFT. Herein, the length of the rising edge is defined as the distance between the first point at which 2% of the final WFT is reached and the point at which 98% of the WFT is reached. After a coating length of 60 mm, the slurry flow is stopped and the falling edge is formed. The falling edge length is the distance between 98% and 2% of the WFT, respectively.

The differences between the edge gradients are shown in detail in **Figure 6** for the rising edge and in **Figure 7** for the falling edge. The rising edges have a similar profile for all the investigated coating speeds. There is a sharp increase in WFT up to the plateau of the final WFT.

Table 2. Overview of coating parameters used for the experiments.

Coating speed [m min^{-1}]	Resulting volume flow [mL min^{-1}]	Coating gap [µm]	WFT [µm]	Theoretical shear rate within the coating gap [s^{-1}]	Capillary number
10	87	161	144.4	1035	0.57
10	158	237	263.6	703	0.64
10	242	416	402.6	401	0.75
20	191	161	159.1	2070	0.92
20	259	237	215.9	1406	1.03
20	468	416	389.8	801	1.22
30	276	161	153.6	3106	1.22
30	372	237	206.8	2110	1.35
30	706	416	392	1202	1.61
50	403	161	134.3	5176	1.74

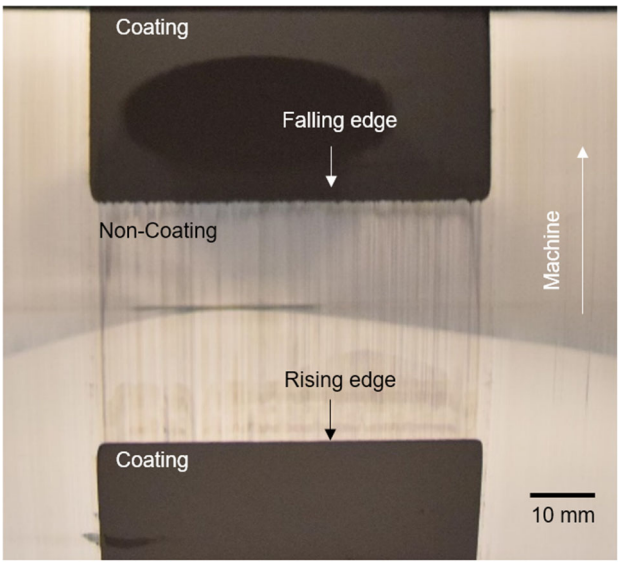

Figure 4. Example of intermittent coating at 20 m min^{-1} including rising edge, falling edge, and a noncoating spacing of 40 mm.

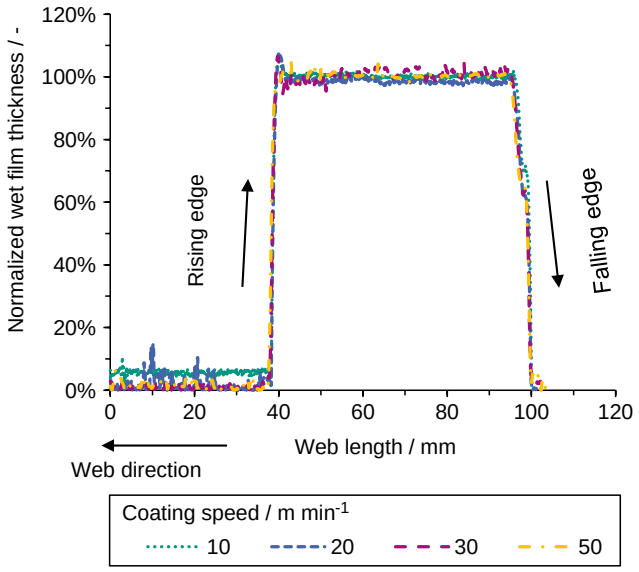

Figure 5. Normalized coating pattern profile with WFT as a function of the coating length with the rising edge on the left-hand side and the falling edge on the right-hand side. The target coating length is 60 mm and the target noncoating length is 40 mm. The WFT is normalized to the thickness plateau of the electrode, as shown in Table 2.

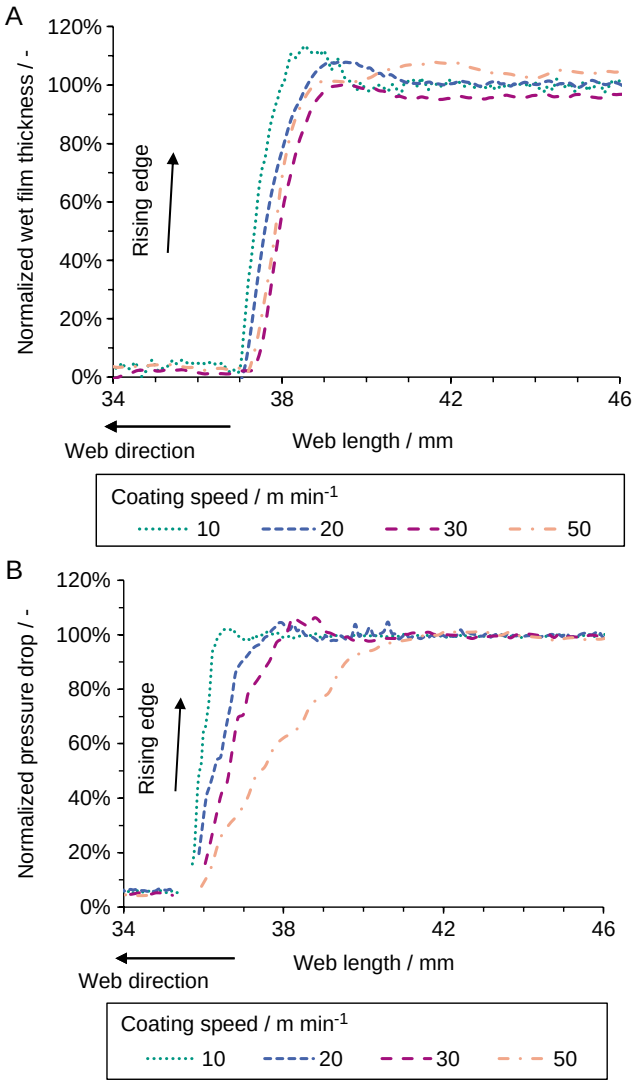

Figure 6. Detailed view of the rising edges for different coating speeds ranging from 10 m min^{-1} to 50 m min^{-1}. A) shows the WFT normalized to the thickness plateau of the electrode shown, as shown in Table 2. B) shows the pressure drop in the slot normalized to the continuous coating pressure drop with resulting distance as horizontal axis. All patterns show a similar inclination with an overshoot after rising for both WFT and pressure drop.

At lower speeds, a wet thickness overshoot can be observed, which is about 7% of the plateau thickness level of about 150 µm (10.3 µm for 10 m min^{-1}, 11.7 µm for 20 m min^{-1}, and 10.0 µm for 30 m min^{-1}). For a higher speed of 50 m min^{-1}, the overshoot decreases to 2.3%, which corresponds to 3.1 µm of the plateau thickness. When comparing the curve with the pressure drop in the slot, as shown in Figure 6B, the same course can be seen. The wet film curve seems to follow the pressure curve at the rising edge. The overshoot at the rising edge is already present in the pressure curve and thus in the volume flow in the slot. The relationship between the pressure gradient and the WFT is described in the study by Schmitt et al.[11]

The falling edges show a characteristic course with an initial slope that merges into an intermediate plateau at a height between 60% and 70% of the plateau thickness. After the intermediate plateau, the film breaks off very steeply. It was found that a homogenous pressure distribution in the coating system is important for the intermittent coating that is similar to the observed pattern.[11] The formation of the intermediate plateau may relate to the emptying of the coating bead, when the flow of slurry from the slot-die is decreasing. In contrast to the findings of Maza and Carvalho,[16]

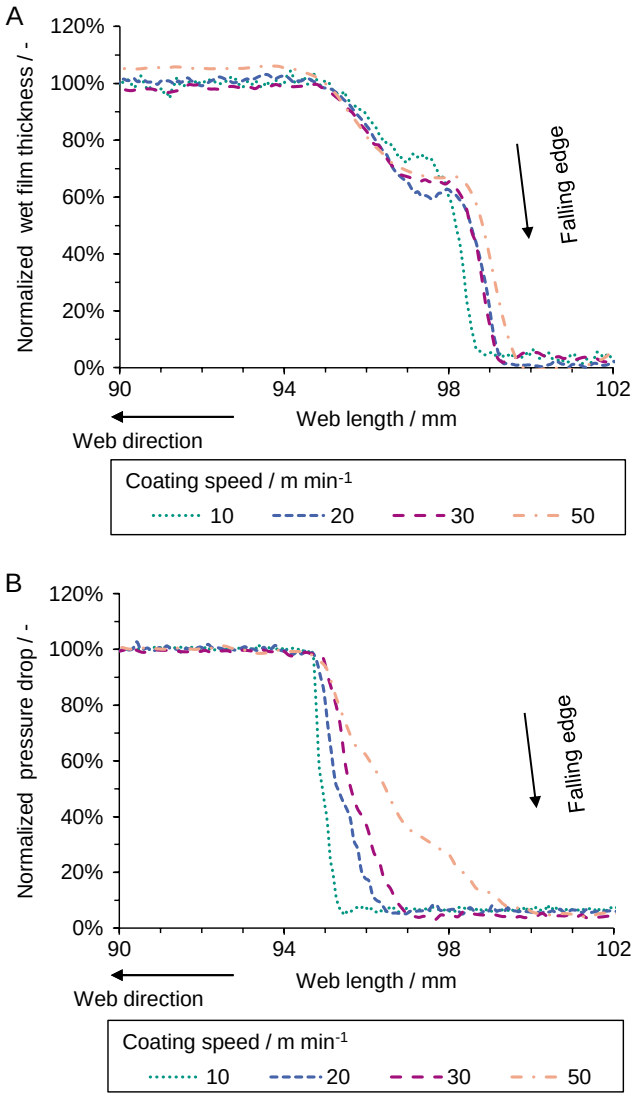

Figure 7. A) Detailed view of the falling edge of WFT and B) pressure drop inside slot for different coating speeds from 10 to 50 m min^{-1}. The WFT is normalized to the thickness plateau of the electrode, as shown in Table 2, and the pressure drop in the slot normalized to the continuous coating pressure drop with resulting distance as horizontal axis.

we observed no super elevation at the falling edge but for this intermediate plateau. A possible mechanism of the formation of the falling edge is shown in **Figure 8**.

The coating of the pattern plateau is comparable with a continuous coating in the steady state (Figure 8A). For interrupting the coating, the valve is switching. Due to the not ideal switching behavior of a technical valve, the volume flow decreases from steady state to zero, as shown in Figure 7B, for the different coating speeds. As the flow decreases, the WFT also decreases (Figure 8B). At the same time, the contact line moves backward and the coating bead between the slot die and the substrate empties (Figure 8C). When the bead empties, the menisci of the liquid bridge between the slot die and the substrate breaks off (Figure 8D). The length of the falling edge not only depends on the volume flow but also on the emptying of the coating bead. This can lead to the higher transmission length for the falling edges compared with the rising edges. The length of the rising edges and falling edges is examined more closely, as shown in **Figure 9**, for the different coating speeds.

Figure 9 shows that the falling edge with a length of 3.6–4.7 mm is significantly longer than the rising edge with a length of 1.1–1.9 mm. This can be explained by the fact that with very short switching times, the emptying of the coating bead is the relevant mechanism for the shape of the falling edge. The geometry and therefore the slurry volume within the coating gap depend on the fixed length of the slot-die lips. This volume is also dependent on the height and width of the coating gap as well as on the width of the slot-die. This volume, which stays the same at all speeds, must be emptied at every coating interruption and thus at every pattern, which explains why the falling edge length is more or less independent of the web speed.

2.4. Influence of WFT on Rising and Falling Edge

Coating of electrodes for high-energy battery cells requires comparably high WFTs, which might be challenging to the intermittent coating process in terms of increased gap volume. To investigate the impact of those high WFTs, the electrode layer is increased from 159 µm (corresponding to 3.4 mAh cm^{-2}) to 210 µm (4.5 mAh cm^{-2}) and up to 390 µm (8.3 mAh cm^{-2}). In **Figure 10**, the influence of the WFT on the rising edge of patterns with a high area loading is shown.

The minimum length of the rising edge was determined at the lowest WFT. The WFT is increased by increasing the volume flow of the slurry to the slot-die and by correspondingly increasing the coating gap. For a coating speed of 20 m min^{-1}, the rising edge length increases in a linear manner from 1.4 mm at 159 µm WFT to 1.7 mm at 216 µm WFT and to 3.6 mm at 390 µm WFT. At a speed of 30 m min^{-1}, the average length of the rising edge is 1.4 mm at 154 µm WFT, 2.0 mm at 207 µm WFT, and 3.5 mm at 392 µm WFT. The length of the rising edge seems to have a linear inclination with increased WFT. By increasing the WFT by the factor of 2.5, the length is increased by the factor of 2.6 at 20 m min^{-1}. At a higher speed of 30 m min^{-1}, the factor for the length is 2.5 as well.

For the rising edge, the film follows the rising volume flow, as mentioned earlier. Since this increase takes longer, the higher the steady-state volume flow is, the formation of the rising edges takes longer and leads to longer edges.

The length of the falling edge is shown in **Figure 11** for the same speeds of 20 and 30 m min^{-1}.

The length of the falling edge slightly increases from 4.3 mm at 159 µm WFT to 4.6 mm at 216 µm WFT and to 5.3 mm at 390 µm WFT at a coating speed of 20 m min^{-1}. For the higher coating speed of 30 m min^{-1}, the falling edge length increases from 4.7 mm at 154 µm WFT to 6.6 mm at 392 µm WFT, with an exception of 4.4 mm at 207 µm WFT. For lower speeds of 20 m min^{-1}, there seems to be a slight increase in the length with a higher film thickness. At the falling edge, the emptying of the coating gap seems to be the dominant factor with increasing film thicknesses, as it has been observed for thin electrode layers, as shown in Figure 7. At this point, differentiation between the impact of

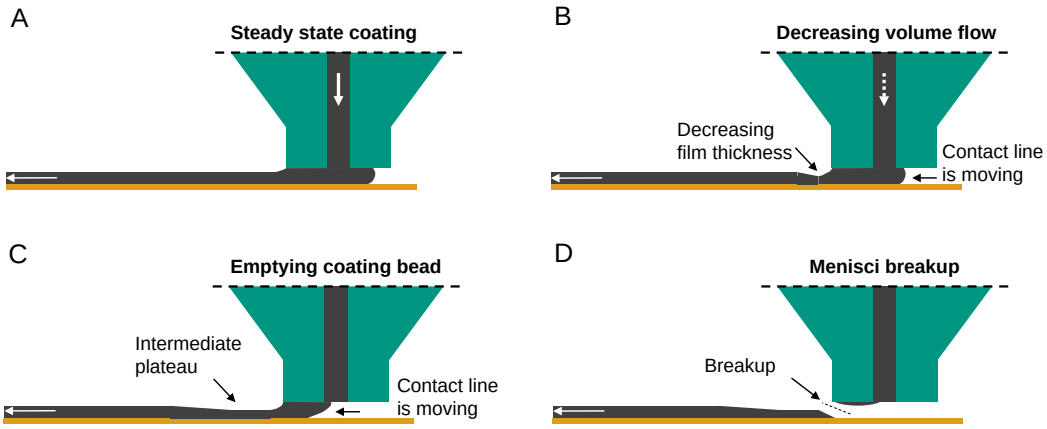

Figure 8. Illustration of the film breakup mechanism at falling edge: A) Steady state coating of plateau. B) Decreasing of volume flow due to valve switching, moving of contact line, and decreasing of film thickness. C) Coating bead is emptying with intermediate plateau. D) Breakup of coating menisci.

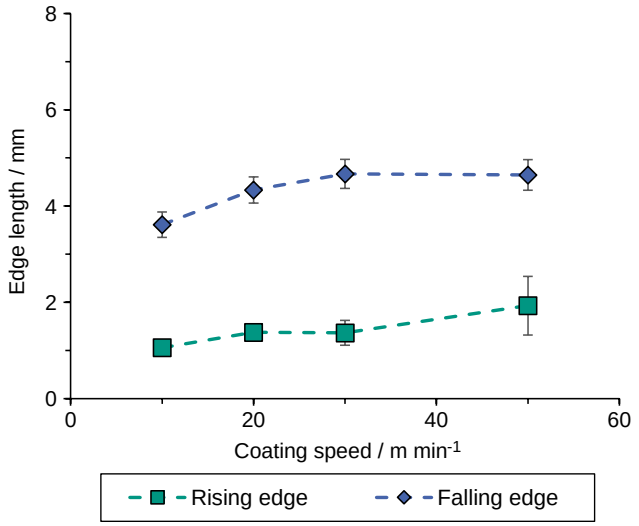

Figure 9. Measure edge lengths of the rising (green, rectangular signs) and the falling edges (blue, diamond signs) in respect to the coating speed.

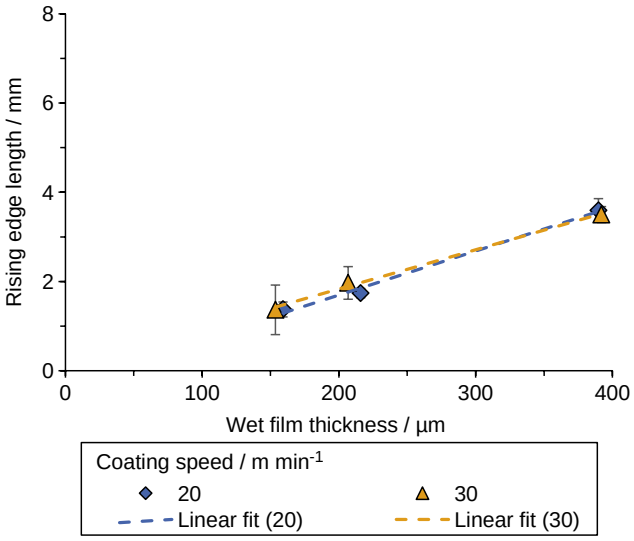

Figure 10. Edge length of the rising edge as a function of the WFT for different coating speeds. The length increases with higher thickness in a proportional manner. A linear fit was used to visualize the dependency.

the film thickness by itself and the influence of the additional residual slurry volume within the coating gap necessary for higher WFT is not possible. sFor the rising edge, the increase in volume of the coating bead, due to larger gaps, is a challenging as well. In this case, it obviously takes longer for the film to reach the WFT plateau height. Compared with the rising edge, as shown in Figure 10, the falling edge is longer in absolute values but with a lower gradient toward higher WFTs. This is also due to the dominant mechanism of the emptying of the coating bead, which is not strongly influenced by the layer thickness.

3. Conclusion

In the presented work, the influence of coating speed and WFT on the rising and falling edge lengths of intermittently coated LIB electrode layers was investigated. A representative such as water-borne and shear-thinning anode slurry was used for the experiments.

The results show that both the rising edge and the falling edge remain their shape even at different coating speeds. The length of the rising edge was observed to be shorter than that of the falling edge. This was valid for the whole range of applied coating speeds and WFTs.

For both edges, the coating speed has only a minor influence. This is explained by the dominant film start-up and break-up mechanisms in the coating bead. The results show that high coating speeds of 50 m min^{-1} are possible for intermittent coating without any drawbacks regarding the pattern edges. When increasing the WFT, the length of the falling edge rises proportionally but with a different gradient for the two adjusted coating

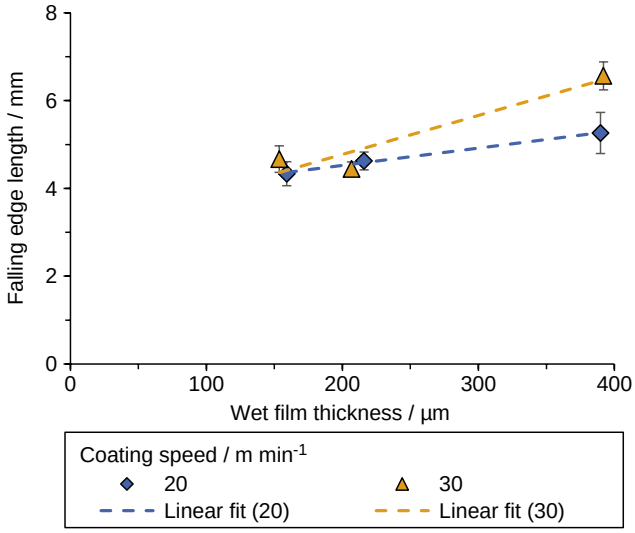

Figure 11. Edge length of the falling edge as a function of the WFT for different coating speeds. A linear fit was used to visualize the dependency.

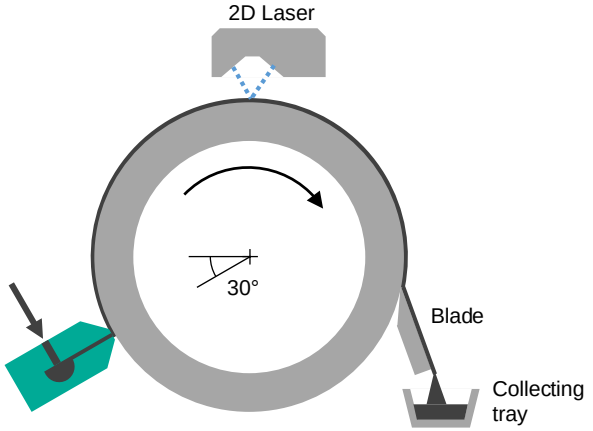

Figure 12. Schematic drawing of the experimental setup with slot-die, roll, and 2D laser triangulation system.

speeds. In contrast, the length of the rising edge increases in a proportional manner for thicker coatings independent of the coating speed. A model mechanism for the formation of the falling edge is presented. Because the coating-bead emptying seems to be the dominant mechanism, the length of the falling edge does not rise linearly with the coating speed.

4. Experimental Section

Anode Materials: The major ingredients in the formulation were slightly flaked graphite (SMG-A, Hitachi) as an active material with an average particle size of 19 µm (D50). The conductive additive was carbon black (Super-P, Timcal). The binder system consisted of the two binders: carboxymethyl cellulose (CMC, Sunrose, Nippon paper industries) and styrene-butadiene rubber (SBR, Zeon).

Anode Slurry Preparation: The anode slurry was prepared by dry mixing of the solids such as graphite and carbon black. The binder and dispersing agent CMC was dissolved in water and gradually added to the solids in three steps. A kneading device (Inoue Mfg, Japan) was used for the mixing steps with dispersing times of 10, 30, and 120 min after dilution steps. After dispersing, the SBR dispersion was added and gently stirred in. The solid content was set to 43% for all the experiments. The viscosity was measured by a rotation viscometer in plate–plate setup with 25 mm diameter (Anton Paar, Germany) from 0.01 to 1000 $1\,s^{-1}$. The return path of the hysteresis measurement was evaluated to get a constant shear history and to exclude any thixotropy effects.

Slot-Die Coating and Coating Setup: The slot-die used for this study consisted of a primary and a secondary distribution cavity. The volume flow for the intermittent coating was interrupted by an intermediate storage inside the die. The process is described in detail earlier[6,10,11,13] and was the same for every experiment in this work. The distance between the slot-die plates was adjusted with a polymer shim of 500 µm thickness. Both lips were astride with a shoulder angle of $\varphi = 90°$ to the coating plane. The dimensionless gap with the ratio of gap distance to WFT was set to be $1.1\,\mu m\,\mu m^{-1}$. A schematic drawing of the coating setup is shown in **Figure 12**.

The slot-die was mounted in 8 o'clock position against a rotating steel roll. On the roll, the coated wet film profile was measured using a 2D laser triangulation system (Keyence LJ-V). Right after analysis of the wet film, the slurry was removed from the roll with a blade for continuous coating trials. For fluid supply, a syringe pump (Cetoni Nexus) was used to set a defined constant volume flow.

Acknowledgements

The authors thank the Federal Ministry of Education and Research (BMBF) for its financial support within the cluster project "ProZell HighEnergy" under the reference number 03XP0073B. This work contributes to the research performed at CELEST (Center for Electrochemical Energy Storage Ulm-Karlsruhe).

Conflict of Interest

The authors declare no conflict of interest.

Keywords

cell stack formation, graphite anodes, intermittent coating, slot-die coating

Received: January 31, 2019
Revised: April 12, 2019
Published online: May 30, 2019

[1] M. Yoshio, R. Brodd, A. Kozawa, *Lithium-Ion Batteries*, Springer, Berlin/New York **2009**.
[2] B. Nykvist, M. Nilsson, *Nat. Clim. Chang.* **2015**, *5*, 329.
[3] A. Thielmann, C. Neef, H. Tim, H. Döscher, M. Wietschel, J. Tübke, Energiespeicher-Roadmap (Update 2017), Fraunhofer ISI **2017**.
[4] J. Kurfer, M. Westermeier, G. Reinhart, Technologies and Systems for Assembly Quality, Productivity and Customization (Hrsg: J. S. Hu) University of Michigan, Ann Arbor **2012**, pp. 33–37.
[5] G. Reinhart, J. Kurfer, *Handhaben in der Batteriefertigung – Forschungs- und Demonstrationszentrum für Lithium-Ionen-Zellen*, Springer-VDI-Verlag, Düsseldorf **2011**, pp. 545–550.
[6] Karlsruher Institut für Technologie. *Elektrodenanordnung, Verfahren zu Ihrer Herstellung und elektrochemische Zelle*. Karlsruher Institut für Technologie, Karlsruhe, Germany **2013**.
[7] D. Mohanty, E. Hockaday, J. Li, D. K. Hensley, C. Daniel, D. L. Wood, *J. Power Sources* **2016**, *312*, 70.

[8] L. David, R. E. Ruther, D. Mohanty, H. M. Meyer, Y. Sheng, S. Kalnaus, C. Daniel, D. L. Wood, *Appl. Energy* **2018**, *231*, 446.
[9] M. Schmitt, K. I. T. Scientific Publishing, Karlsruhe, Germany **2015**.
[10] C. K. Yang, D. S. H. Wong, T. J. Liu, *Coat. Res. Assoc.* **2004**, *5*, 43.
[11] M. Schmitt, R. Diehm, P. Scharfer, W. Schabel, *J. Coat. Technol. Res.* **2015**, *12*, 927.
[12] I. de Vries, Presentation ISCST, San Diego, CA, USA **2014**.
[13] R. Diehm, M. Schuster, M. Schmitt, P. Scharfer, W. Schabel, ISCST, Long Beach, CA, USA, **2016**.
[14] R. Diehm, J. Kumberg, P. Scharfer, W. Schabel, ISCST, Pittsburg, PA, USA, **2018**.
[15] Y.-R. Chang, C.-F. Lin, T.-J. Liu, *Polym. Eng. Sci.* **2009**, *49*, 1158.
[16] D. Maza, M. S. Carvalho, *Polym. J. Coat. Technol. Res.* **2017**, *14*, 1003.